

EXPLORING NUCLEON-NUCLEON CORRELATIONS IN $(e, e'NN)$ REACTIONS

H. MÜTHER

Institut für Theoretische Physik,
Universität Tübingen, Germany

November 20, 2018

Abstract

Correlations in the nuclear wave-function beyond the mean-field or Hartree-Fock approximation are very important to describe basic properties of nuclear structure. Attempts are made to explore details of these correlations in exclusive nucleon knock-out by electron scattering experiments. Basic results of $(e, e'p)$ experiments are reviewed. The role of correlations in $(e, e'NN)$ experiments is discussed. Special attention is paid to a consistent description of the competing effects due to final state interaction, meson exchange current and isobar currents. Results are discussed for systematic studies of these features in nuclear matter as well as for specific examples for the finite nucleus ^{16}O .

1 NN Correlations

Nuclei are a very intriguing object to explore the theory of quantum-many-body systems. One of the reasons is that realistic wave functions of nuclear systems must exhibit strong two-particle correlations. This can be demonstrated in a little ‘theoretical experiment’: Assuming a realistic model for the nucleon-nucleon (NN) interaction[1, 2, 3, 4, 5], this means an interaction which reproduces the empirical data of NN scattering below the pion threshold, one may calculate the energy of nuclear matter within the mean field or Hartree-Fock approximation. Results of such a calculation are listed in the first row of table 1. One finds that all these interactions yield a positive value for the energy per nucleon, which means that nuclear matter as well as all nuclei would be unbound. Only after the effects of two-body correlations are included, one obtains a value which is in rough agreement with the empirical value of -16 MeV per nucleon. This demonstrates that nuclear correlations are indispensable to describe the structure of nuclei.

	CDB	ArgV18	Nijm1	Bonn C	Reid
E_{HF}	4.64	30.34	12.08	29.56	176.20
E_{Corr}	-17.11	-15.85	-15.82	-14.40	-12.47
$V_{\pi HF}$	16.7	15.8	15.0	17.8	
$V_{\pi Corr}$	-2.30	-40.35	-28.98	-45.74	
T	36.23	47.07	39.26	40.55	49.04

Table 1: Energy per nucleon for nuclear matter at the empirical saturation density. Results are displayed for the NN interactions CDB [1], ArgV18 [2], Nijm1 [3], Bonn C [4] and the Reid potential [5]. The results obtained in the Hartree-Fock approximation E_{HF} are compared to those of Brueckner-Hartree-Fock calculations (E_{Corr}). Furthermore the contribution of the π exchange to the total energy in Born approximation ($V_{\pi HF}$) and including the effects of correlations ($V_{\pi Corr}$) as well as the expectation value of the kinetic energy (T) are listed. All entries are given in MeV.

In order to explore dominant components of these correlation, table 1 also lists the expectation value of the π -exchange contribution to the NN interaction using the HF approximation ($V_{\pi HF}$) and with inclusion of the correlation effects ($V_{\pi Corr}$). One finds that the gain in binding energy is not only due to the central short-range correlation effects, i.e. the nuclear wave function tries to minimize the probability that two nucleons approach each other so close that they feel the repulsive core of the interaction. A large part of this gain in binding energy is due to pionic correlations which are dominated by the effects of the tensor force.

The different interaction models all reproduce the same empirical NN scattering phase shifts. This is true in particular for the modern NN interactions: the charge-dependent Bonn potential (CDB)[1], the Argonne V18 (ArgV18)[2] and the Nijmegen interaction (Nijm1)[3], which all yield an excellent fit of the same phase shifts. Nevertheless, they predict quite different correlations. This can be seen e.g. from inspecting the expectation values for the kinetic energies per nucleon (denoted as T in table 1). This means that correlations are a significant fingerprint of the interaction of two nucleons in a nuclear medium. So if we find a way to measure details of these correlations, we shall obtain information on the validity of the various models for the NN interaction.

2 Correlations and exclusive $(e, e'p)$ reactions

The uncorrelated Hartree-Fock state of nuclear matter is given as a Slater determinant of plane waves, in which all states with momenta k smaller than the Fermi momentum k_F are occupied, while all others are completely unoccupied.

Correlation in the wave function beyond the mean field approach will lead to occupation of states with k larger than k_F . Therefore correlations should be reflected in an enhancement of the momentum distribution at high momenta. Indeed, microscopic calculations exhibit such an enhancement for nuclear matter as well as for finite nuclei[6, 7]. One could try to measure this momentum distribution by means of exclusive $(e, e'p)$ reactions at low missing energies, such that residual nucleus remains in the ground state or other well defined bound state. From the momentum transfer q of the scattered electron and the momentum p of the outgoing nucleon one can calculate the momentum of the nucleus before the absorption of the photon and therefore obtain direct information on the momentum distribution of the nucleons inside the nucleus.

This idea, however, suffers from a little inaccuracy. To demonstrate this we write the momentum distribution $n(k)$ representing the ground state wave function of the target nucleus by Ψ_A , denoting the creation (annihilation) operator for a nucleon with momentum k by a_k^\dagger (a_k), as

$$\begin{aligned} n(k) &= \langle \Psi | a_k^\dagger a_k | \Psi \rangle \\ &= \int_0^\infty dE \langle \Psi | a_k^\dagger | \Phi_{A-1}(E) \rangle \langle \Phi_{A-1}(E) | a_k | \Psi \rangle \\ &= \int_0^\infty dE S(k, E) \\ \text{with } S(k, E) &= \left| \langle \Psi | a_k^\dagger | \Phi_{A-1}(E) \rangle \right|^2. \end{aligned}$$

In the second line of this equation we have inserted the complete set of eigenstates for the residual nucleus with $A - 1$ nucleons and excitation energy E . Therefore, if one performs an exclusive $(e, e'p)$ experiment leading to the residual nucleus in its ground state, one does not probe the momentum distribution but the spectral function at an energy $E = 0$. While the total momentum distribution exhibits the enhancement at high momenta discussed above, the spectral function at small energies does not have this feature[6] and the momentum distribution extracted from such experiments is very similar to the one derived from Hartree-Fock wave functions.

This is demonstrated by Figure 1, which compares experimental data of $(e, e'p)$ experiments on ^{16}O leading to the ground state of the residual nucleus ^{15}N , which were performed at MAMI in Mainz[8], with theoretical calculations[9]. The calculation account for the final state interaction of the outgoing nucleon with the residual nucleus by means of a relativistic optical potential. One finds that the spectral function calculated with inclusion of correlation yields the same shape as the corresponding Hartree-Fock approximation. The only difference being the global normalization: the spectroscopic factor.

Therefore exclusive $(e, e'p)$ reactions yield a rather limited amount of information on correlation effects, they are sensitive to the mean field properties of the nuclear system. There is a major discussion of these mean field prop-

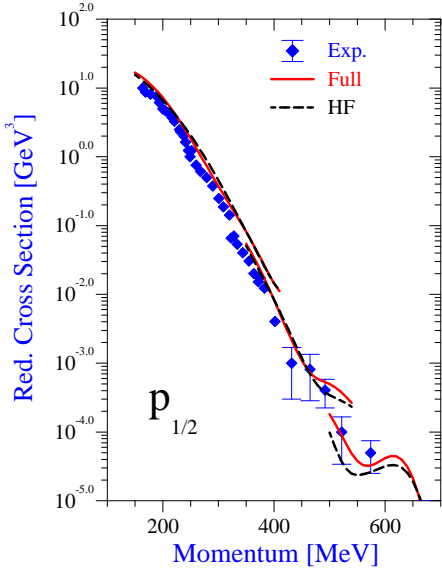


Figure 1: Reduced cross section for the $^{16}\text{O}(e, e'p)^{15}\text{N}$ reaction leading to the ground state ($1/2^-$) of ^{15}N in the kinematical conditions considered in the experiment at MAMI (Mainz) [8]. Results for the mean-field description (HF) and the fully correlated spectral function (Full) are presented.

erties in nuclear physics: Motivated by the success of the Walecka model[10], attempts have been made to include relativistic features in microscopic nuclear many-body studies. Such attempts are often referred to as Dirac-Brueckner-Hartree-Fock calculations[11, 12]. The main prediction of these relativistic nuclear structure calculations is that the small component of the Dirac spinors for the nucleon inside a nucleus is enhanced relative to the small component of a free nucleon with the same momentum. This enhancement can be parameterized in terms of an effective Dirac mass m^* which is significantly smaller than the bare nucleon mass.

Can one observe this enhancement of the small component of the Dirac spinor by means of $(e, e'p)$ experiments? Theoretical calculations predict that this may be possible, if one performs a more detailed analysis of the corresponding cross section. For that purpose one decomposes the cross section into a contraction of hadronic responses and the appropriate electron contributions, which are

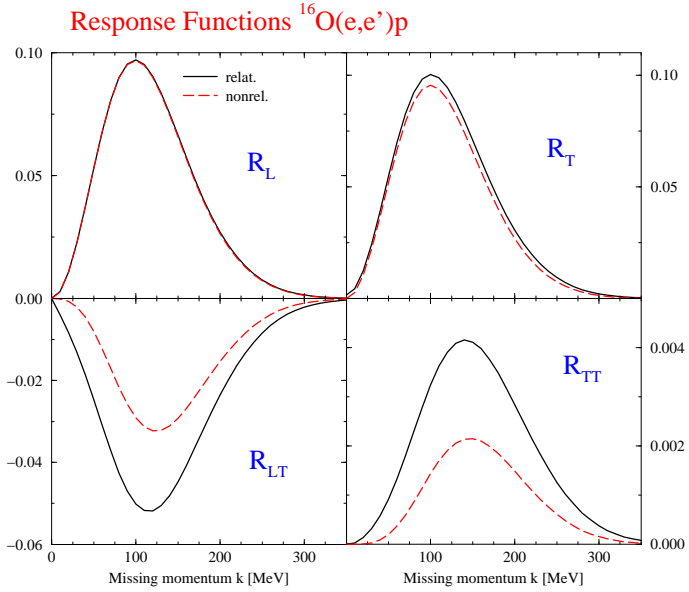


Figure 2: Response functions R_L , R_T , R_{LT} and R_{TT} for the knockout of a nucleon from $p_{1/2}$ state in ^{16}O as a function of the missing momentum. Comparison of relativistic and non-relativistic approach

defined as in [13]

$$\frac{m|p_x|}{(2\pi)^3} \sigma_{Mott} (V_L R_L + V_T R_T + V_{LT} R_{LT} \cos \phi + V_{TT} R_{TT} \cos 2\phi) .$$

Results for the hadronic response functions with and without the relativistic effect[14] are displayed in Figure 2. While the relativistic features do not effect the longitudinal R_L and transverse repons functions R_T , they predict an enhancement of the interference structure functions R_{LT} and R_{TT} as compared to the non-relativistic reduction. This feature is discussed more in detail by Moya de Guerra and Udias[15]. First experimental results on R_{LT} are presented by Bertozi[16] at this workshop.

3 Kinematical study of $(e, e'NN)$ in nuclear matter

As exclusive one-nucleon knock-out experiments only yield limited information on NN correlations, one may try to investigate exclusive $(e, e'NN)$ reactions,

i.e. triple coincidence experiments in which the energies of the two outgoing nucleons and the energy of the scattered electron guarantee that the rest of the target nucleus remains in the ground state or a well defined excited state. The idea that processes in which the virtual photon, produced by the scattered electron, is absorbed by a pair of nucleons should be sensitive to the correlations between these two nucleons.

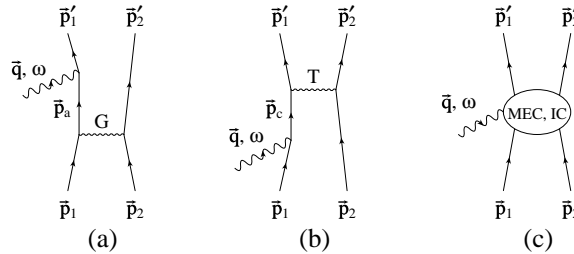


Figure 3: Diagrams for the different processes contributing to the $(e, e' 2N)$ reaction. Diagram (a) and (b) show the absorption of the photon by a single nucleon. The nucleon-nucleon correlations are described by the G matrix. Diagram (c) depicts photon absorption via meson exchange (MEC) or isobaric currents (IC)

Unfortunately, however, this process which is represented by the diagram in Figure 3a, competes with the other processes described by the diagrams of Figure 3b and c. These last two diagrams refer to the effects of final-state-interaction (FSI) and contributions of two-body currents. Here we denote by final state interaction not just the feature that each of the outgoing nucleons feels the remaining nucleus in terms of an optical potential. Here we call FSI the effect, that one of the nucleons absorbs the photon, propagates (on or off-shell) and then shares the momentum and energy of the photon by interacting with the second nucleon which is also knocked out the target. The processes described in Figures 3a and 3b, correlations and FSI, are rather similar, they differ only by the time ordering of NN interaction and photon absorption. Therefore it seems evident that one must consider both effects in an equivalent way. Nevertheless, all studies up to now have ignored this equivalency but just included the correlation effect in terms of a correlated two-body wave function. In our approach we will assume the same interaction to be responsible for the correlations and the FSI, correlations are evaluated in terms of the Brueckner G -matrix[17], while the T -matrix derived from the very same interaction is used to determine FSI.

The two-body current contributions of Figure 3c include Meson Exchange Current (MEC) and Isobar Current (IC) contributions. The MEC effects should be calculated consistently with the meson exchange terms included in the NN

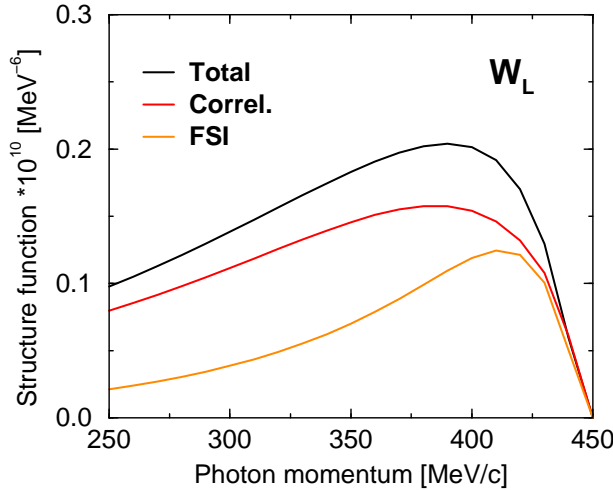


Figure 4: Longitudinal structure function for the knockout of a proton-proton pair in a 'super parallel' kinematical situation with angles $\theta'_{p,1} = 0^\circ$ and $\theta'_{p,2} = 180^\circ$ of the two protons with respect to the direction of the photon momentum. The figure has been generated assuming final kinetic energies $T_{p,1} = 156$ MeV and $T_{p,2} = 33$ MeV of the two protons. The structure function is displayed as a function of the photon momentum, keeping the photon energy constant at $\omega = 215$ MeV

interaction, used to calculate correlations and FSI. In our calculations up to day we only account for the contributions due to the exchange of the pions. Note that the pion-seagull and pion in flight term only contribute if the emitted pair contains a proton and a neutron. Contributions of other charged mesons like e.g. the ρ meson have been considered e.g. by Vanderhaeghen et al. [18] and shall also be included in future investigations.

The IC contributions contain diagrams like the ones displayed in Figures 3a and b. The only difference being that the intermediate nucleon line is replaced by the propagation of the Δ excitation. This demonstrates that also IC contributions should be treated in terms of baryon-baryon interactions accounting for admixture of Δ configurations to the target wave functions as well as FSI effects with intermediate isobar terms. Presently the IC terms are evaluated in terms of the Born diagrams, including again only π exchange for the transition interactions $NN \rightleftarrows N\Delta$. Also in this case one should account for the effects of the ρ exchange.

In this section I would like to present results for the various contributions just introduced, calculated for nuclear matter at saturation density. Of course, this study will not lead to any result, which can directly be compared with

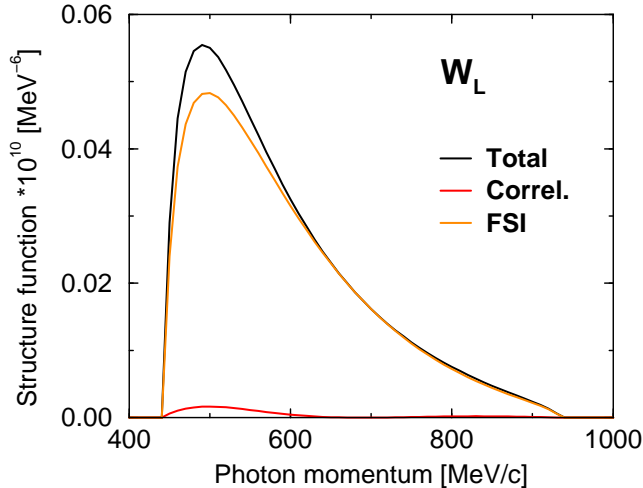


Figure 5: Longitudinal structure function for $(e, e'pp)$ with $\omega = 230$ MeV, assuming $\theta_{p_i} = \pm 30^\circ$ and $T_{p,i} = 70$ MeV

experimental data for a specific target nucleus. The idea is to get some general features, which are independent on the specific target nucleus or final state of the residual nucleus. We would like to see, if we can provide general information about the importance of the various contributions just discussed. It is the hope, that one may find special kinematical situations, in which one of the contributions mentioned above is dominating over others. All results discussed here have been obtained with the Bonn A potential defined by Machleidt[4]. Details of these calculations are described in reference[17].

As a first example we consider the longitudinal structure function for the knockout of a proton-proton pair. One of the protons is emitted parallel to the momentum of the virtual photon with an energy of $T_{p,1} = 156$ MeV, while the second is emitted antiparallel to the photon momentum with an energy of $T_{p,2} = 33$ MeV (see Figure 4). This is called the ‘super-parallel kinematic’, which should be appropriate for a separation of longitudinal and transverse structure functions. In this situation the dominant contribution to the longitudinal response function is due to correlation effects (red curve). But also the FSI effects contribute in a non-negligible way to the cross section (yellow curve), although the two protons are emitted in opposite directions.

The effects of FSI are much more important, if we request that the two protons are emitted in a more symmetric way. As an example we show the longitudinal structure function for $(e, e'pp)$, requesting that each of the protons carries away an energy of 70 MeV and is emitted with an angle of 30° or -30°

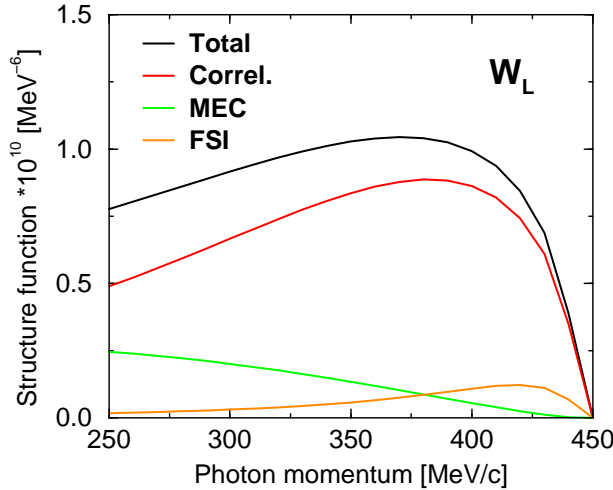


Figure 6: Longitudinal structure function for $(e, e'pn)$ for the kinematical condition as displayed in Figure 4

with respect to the momentum transfer q of the virtual photon. Corresponding results are displayed in Figure 5. For this kinematical situation the FSI contribution is much more important than the correlation effect.

As a last example we present the results for the longitudinal structure function for the $(e, e'pn)$ reaction, assuming the same kinematical (super-parallel) setup as has been employed for the $(e, e'pp)$ reaction displayed in Figure 4. The resulting structure function for $(e, e'pn)$ displayed in Figure 6 is almost an order of magnitude larger than for the corresponding $(e, e'pp)$ case. In $(e, e'pn)$ reactions one has also to include the effects of MEC. Note, however, that for the case considered the MEC contribution are smaller than the correlation effects. This is due to a strong cancellation between the pion seagull and the pion in flight contributions to the MEC. The dominating contribution to the longitudinal response is again the correlation part. Comparison with Figure 4 demonstrates that the pn correlations are significantly larger than those for the pp pairs. This supports our conclusion from discussing the results of table 1 that the pionic or tensor correlations which are different for isospin $T = 0$ and $T = 1$ pairs play an important role and are even more important than the central correlations, which are independent of the isospin.

More detailed results including the transversal structure function and the effect of isobar currents have partly been published already in [17]. The discussion of further results is in preparation[19]

4 Correlations in finite nuclei

Various quite different approaches have been developed to determine correlations in the nuclear wave function, which are beyond the mean-field or Hartree-Fock approach. In the preceding section we have employed a calculation of correlation effects in terms of the Brueckner G-matrix. In this section we will consider the so-called coupled cluster or “ $\exp(S)$ ” method. The basic features of the coupled cluster method have been described already in the review article by Kümmel et al. [20]. More recent developments and applications can be found in [21]. Here we will only present some basic equations. The many-body wave function of the coupled cluster or $\exp(S)$ method can be written

$$|\Psi\rangle = \exp\left(\sum_{n=1}^A \hat{S}_n\right) |\Phi\rangle. \quad (1)$$

The state $|\Phi\rangle$ refers to the uncorrelated model state, which we have chosen to be a Slater determinant of harmonic oscillator functions with an oscillator length $b=1.72$ fm, which is appropriate for the description of our target nucleus ^{16}O . The linked n -particle n -hole excitation operators can be written

$$\hat{S}_n = \frac{1}{n!2} \sum_{\nu_i \rho_i} < \rho_1 \dots \rho_n | S_n | \nu_1 \dots \nu_n > a_{\rho_1}^\dagger \dots a_{\rho_n}^\dagger a_{\nu_n} \dots a_{\nu_1}. \quad (2)$$

Here and in the following the sum is restricted to oscillator states ρ_i which are unoccupied in the model state $|\Phi\rangle$, while states ν_i refer to states which are occupied in $|\Phi\rangle$. For the application discussed here we assume the so-called S_2 approximation, i.e. we restrict the correlation operator in (1) to the terms with \hat{S}_1 and \hat{S}_2 . One may introduce one- and two-body wave functions

$$\begin{aligned} \psi_1 | \nu_1 > &= | \nu_1 > + \hat{S}_1 | \nu_1 > \\ \psi_2 | \nu_1 \nu_2 > &= \mathcal{A} \psi_1 | \nu_1 > \psi_1 | \nu_2 > + \hat{S}_2 | \nu_1 \nu_2 > \end{aligned} \quad (3)$$

with \mathcal{A} denoting the operator antisymmetrizing the product of one-body wave functions. Using these definitions one can write the coupled equations for the evaluation of the correlation operators \hat{S}_1 and \hat{S}_2 in the form

$$< \alpha | \hat{T}_1 \psi_1 | \nu > + \sum_{\nu_1} < \alpha \nu_1 | \hat{T}_2 \hat{S}_2 + \hat{V}_{12} | \nu \nu_1 > = \sum_{\nu_1} \epsilon_{\nu_1 \nu} < \alpha | \psi_1 | \nu_1 >, \quad (4)$$

where \hat{T}_i stands for the operator of the kinetic energy of particle i and \hat{V}_{12} is the two-body potential. Furthermore we introduce the single-particle energy matrix defined by

$$\epsilon_{\nu_1 \nu} = < \nu_1 | \hat{T}_1 | \nu > + \sum_{\nu'} < \nu_1 \nu' | \hat{V}_{12} \psi_2 | \nu \nu' > \quad (5)$$

The Hartree-Fock type equation (4) is coupled to a two-particle equation of the form

$$0 = \langle \alpha\beta | \hat{Q} \left[(\hat{T}_1 + \hat{T}_2) \hat{S}_2 + \hat{V}_{12} \psi_2 + \hat{S}_2 \hat{P} \hat{V}_{12} \psi_2 \right] | \nu_1 \nu_2 \rangle - \sum_{\nu} \left(\langle \alpha\beta | \hat{S}_2 | \nu \nu_2 \rangle \epsilon_{\nu \nu_1} + \langle \alpha\beta | \hat{S}_2 | \nu_1 \nu \rangle \epsilon_{\nu \nu_2} \right) \quad (6)$$

In this equation we have introduced the Pauli operator \hat{Q} projecting on two-particle states, which are not occupied in the uncorrelated model state $|\Phi\rangle$ and the projection operator \hat{P} , which projects on two-particle states, which are occupied. If for a moment we ignore the term in (4) which is represented by the operators $\hat{T}_2 \hat{S}_2$ and also the term in (6) characterized by the operator $\hat{S}_2 \hat{P} \hat{V}_{12}$ the solution of these coupled equations corresponds to the Brueckner-Hartree-Fock approximation and we can identify the matrix elements of $\hat{V}_{12} \psi_2$ with the Brueckner G -matrix. Indeed the effects of these two terms are rather small and we have chosen the coupled cluster approach mainly because it provides directly correlated two-body wave functions (see eq.3). More details about the techniques which are used to solve the coupled cluster equations can be found in [22, 23].

As an example we would like to present the effects of correlations on the two-body density obtained by removing two protons from oscillator $p_{1/2}$ states, coupled to total angular momentum $J = 0$ and isospin $T = 1$

$$| \langle \vec{r}_1 \vec{r}_2 | \psi_2 | p_{1/2}, p_{1/2} J = 0, T = 1 \rangle |^2 \quad (7)$$

In Figure 7 this two-body density is displayed for a fixed $\vec{r}_1 = (x_1 = 0, y_1 = 0, z_1 = 2 \text{ fm})$ as a function of \vec{r}_2 , restricting the presentation to the x_2, z_2 half-plane with $(x_2 > 0, y_2 = 0)$. The upper part of this figure displays the two-body density without correlations ($\hat{S}_2 = 0$). One observes that the two-body density, displayed as a function of the position of the second particle \vec{r}_2 is not affected by the position of the first one \vec{r}_1 . Actually, the two-body density displayed is equivalent to the one-body density. This just reflects the feature of independent particle motion. If correlation effects are included, as it is done in the lower part of Figure 7, one finds a drastic reduction of the two-body density at $\vec{r}_2 = \vec{r}_1$ accompanied by a slight enhancement at medium separation between \vec{r}_1 and \vec{r}_2 .

In order to amplify the effect of correlations, Figure 8 displays the corresponding correlation densities (i.e. replace ψ_2 by \hat{S}_2 , see also (3)). While the upper part shows the correlation density for the removal of a proton-proton pair, the corresponding density for a proton-neutron pair is displayed in the lower part. Comparing these figures one sees that the pn correlations are significantly stronger than the pp correlations. This is mainly due to the presence of pionic or tensor correlations in the case of the pn pair. Figure 8 also exhibits quite nicely the range of the correlations. This range is short compared to the size of the nucleus even in the case of the pn correlations. All results

displayed in this section have been obtained using the Argonne V14 potential for the NN interaction[24].

5 Two nucleon knockout on ^{16}O

The coincidence cross section for the reaction induced by an electron with momentum \vec{p}_0 and energy E_0 , with $E_0 = |\vec{p}_0| = p_0$, where two nucleons, with momenta \vec{p}'_1 , and \vec{p}'_2 and energies E'_1 and E'_2 , are ejected from a nucleus is given, in the one-photon exchange approximation and after integrating over E'_2 , by [25]

$$\frac{d^8\sigma}{dE'_0 d\Omega dE'_1 d\Omega'_1 d\Omega'_2} = K \Omega_f f_{\text{rec}} |j_\mu J^\mu|^2. \quad (8)$$

In Eq. (8) E'_0 is the energy of the scattered electron with momentum \vec{p}'_0 , $K = e^4 p'_0 / 4\pi^2 Q^4$ where $Q^2 = \vec{q}^2 - \omega^2$, with $\omega = E_0 - E'_0$ and $\vec{q} = \vec{p}_0 - \vec{p}'_0$, is the four-momentum transfer. The quantity $\Omega_f = p'_1 E'_1 p'_2 E'_2$ is the phase-space factor and integration over E'_2 produces the recoil factor

$$f_{\text{rec}}^{-1} = 1 - \frac{E'_2}{E_B} \frac{\vec{p}'_2 \cdot \vec{p}_B}{|\vec{p}'_2|^2}, \quad (9)$$

where E_B and \vec{p}_B are the energy and momentum of the residual nucleus. The cross section is given by the square of the scalar product of the relativistic electron current j^μ and of the nuclear current J^μ , which is given by the Fourier transform of the transition matrix elements of the charge-current density operator between initial and final nuclear states

$$J^\mu(\vec{q}) = \int <\Phi_f | \hat{J}^\mu(\vec{r}) | \Phi_i> e^{i\vec{q} \cdot \vec{r}} d\vec{r}. \quad (10)$$

If the residual nucleus is left in a discrete eigenstate of its Hamiltonian, i.e. for an exclusive process, and under the assumption of a direct knockout mechanism, Eq. (10) can be written as [25]

$$\begin{aligned} J^\mu(\vec{q}) = & \int \phi_f^*(\vec{r}_1 \sigma_1, \vec{r}_2 \sigma_2) J^\mu(\vec{r}, \vec{r}_1 \sigma_1, \vec{r}_2 \sigma_2) \phi_i(\vec{r}_1 \sigma_1, \vec{r}_2 \sigma_2) \\ & \times e^{i\vec{q} \cdot \vec{r}} d\vec{r} d\vec{r}_1 d\vec{r}_2 d\sigma_1 d\sigma_2. \end{aligned} \quad (11)$$

Eq. (11) contains three main ingredients: the two-nucleon overlap integral ϕ_i , the nuclear current J^μ and the final-state wave function ϕ_f .

In the model calculations the final-state wave function ϕ_f includes the interaction of each one of the two outgoing nucleons with the residual nucleus while their mutual interaction, which we have discussed as FSI in the preceding section is here neglected. Therefore, the scattering state is written as the

product of two uncoupled single-particle distorted wave functions, eigenfunctions of a complex phenomenological optical potential which contains a central, a Coulomb and a spin-orbit term.

The nuclear current operator in Eq. (11) is the sum of a one-body and a two-body part. In the one-body part convective and spin currents are included. As discussed already in section 3, the two-body current includes, the seagull and pion-in-flight diagrams and the diagrams with intermediate isobar configurations.

The two-nucleon overlap integral ϕ_i contains the information on nuclear structure and allows one to write the cross section in terms of the two-hole spectral function. For a discrete final state of the ^{14}N nucleus, with angular momentum quantum number J , the state ϕ_i is expanded in terms of the correlated two-hole wave functions defined in the preceding section as

$$\phi_i^{JT}(\vec{r}_1\sigma_1, \vec{r}_2\sigma_2) = \sum_{\nu_1\nu_2} a_{\nu_1\nu_2}^{JT} \langle \vec{r}_{12}, \vec{R}, \sigma_1, \sigma_2 | \psi_2 | \nu_1\nu_2 JT \rangle \quad (12)$$

The expansion coefficients $a_{\nu_1\nu_2}^{JT}$ are determined from a configuration mixing calculations of the two-hole states in ^{16}O , which can be coupled to the angular momentum and parity of the requested state. The residual interaction for this shell-model calculation is also derived from the Argonne V14 potential and corresponds to the Brueckner G-matrix. Note that these expansion coefficients $a_{\nu_1\nu_2}^{JT}$ account for the global or long-range structure of the specific nuclear states, while the information on short-range correlations is already contained in $\langle \vec{r}_{12}, \vec{R}, \sigma_1, \sigma_2 | \psi_2 | \nu_1\nu_2 JT \rangle$.

Results for the cross section of exclusive $(e, e'pn)$ reactions on ^{16}O leading to the ground state of ^{14}N are displayed in Figure 9. The calculations have been performed in the super-parallel kinematic, which we already introduced before. The kinematical parameters correspond to those adopted in a recent $^{16}\text{O}(e, e'pp)^{14}\text{C}$ experiment at MAMI [27]. In order to allow a direct comparison of $(e, e'pp)$ with $(e, e'pn)$ experiments, the same setup has been proposed for the first experimental study of the $^{16}\text{O}(e, e'pn)^{14}\text{N}$ reaction [28]. This means that we assume an energy of the incoming electron $E_0 = 855$ MeV, electron scattering angle $\theta = 18^\circ$, $\omega = 215$ MeV and $q = 316$ MeV/c. The proton is emitted parallel and the neutron antiparallel to the momentum transfer \vec{q} .

Separate contributions of the different terms of the nuclear current are shown in the figure and compared with the total cross section[23]. The contribution of the one-body current, entirely due to correlations, is large. It is of the same size as that of the pion seagull current. The contribution of the Δ -current is much smaller at lower values of p_B , whereas for values of p_B larger than 100 MeV/c it becomes comparable with that of the other components. It is worth noting the the total cross section is about an order of magnitude larger than the one evaluated for the corresponding $(e, e'pp)$ experiment[29]. This confirms our finding about the relative cross sections for pp and pn knock out, which we have observed already in section 3.

In Fig. 10 the same quantities as in Fig. 9 are shown, but the two-nucleon overlap has been calculated with the simpler prescription of correlations, i.e. by the product of the pair function of the shell model, described for 1_1^+ as a pure $(p_{1/2})^{-2}$ hole, and of a Jastrow type central and state independent correlation function. The large differences between the cross sections in Figs. 9 and 10 indicate that a refined description of the two-nucleon overlap, involving a careful treatment of both aspects related to nuclear structure and NN correlations, is needed to give reliable predictions of the size and the shape of the $(e, e'pn)$ cross section.

The cross sections for the transition to the excited 1_2^+ state are displayed in Figs. 11. The two-nucleon overlap function for this state contains the same components in terms of relative and c.m. wave functions and the same defect functions as for the 1_1^+ ground state, but they are weighed with different amplitudes $a_{\nu_1 \nu_2}^J$ in Eq. (12). In practice the two overlap functions have different amplitudes for $p_{1/2}$ and $p_{3/2}$ holes. This has the consequence that the cross sections in Figs. 9 and 11 have a different shape and are differently affected by the various terms of the nuclear current. So transition to various states probe the ingredients of the transient matrix elements in different ways. More details will be presented in the contribution of Carlotta Giusti[30].

6 Conclusion

It has been the aim of this contribution to demonstrate that exclusive $(e, e'NN)$ reactions are sensitive to NN correlations and therefore sensitive to the NN interaction in the nuclear medium at short inter-nucleon distances. The careful study and analysis of these reactions is a challenge for experimental but also theoretical efforts. In particular it should be pointed out:

- pp as well as pn knock-out experiments should be performed. The cross sections for pn knock-out are significantly larger than for corresponding pp emission. This is partly due to the meson-exchange-current (MEC) contributions for the charged mesons, which is absent in pp knock-out. The difference, however, also reflects the isospin dependence of nuclear correlations. While the study of $(e, e'pp)$ mainly explores the short-range central correlations, the corresponding $(e, e'pn)$ experiments also probe tensor correlations.
- Effects of Final State Interaction (FSI) are non-negligible. Most of the studies up to now consider FSI effects only in a mean field approach. It must be emphasized, however, that the residual interaction between the two ejected nucleons has a non-negligible effect as well. This is even true, when the two nucleons are emitted ‘back - to - back’. FSI effects, however, get much more important for other final states.

- All contributions to the $(e, e'NN)$ cross section should be determined in a consistent way. In order to separate the various contributions, one should try to separate the various structure functions (longitudinal and transverse). One may also take advantage of the fact that transitions to various final states in the residual nucleus probe the different contributions differently.
- The super-parallel kinematic seems to be quite appropriate for the study of correlation effects.

Acknowledgments

The results, which have been presented here, have been obtained in collaborations with many colleagues. In particular I would like to mention the PhD students Daniel Knödler, Markus Stauf and Stefan Ulrych. Furthermore, I would like to thank K. Allaart, K. Amir-Azimi-Nili, P. Czerski, W.H. Dickhoff, C. Giusti, F.D. Pacati, A. Polls and J. Udias. This work has been supported by grants from the DFG (SFB 382, GRK 135 and Wa728/3).

References

- [1] R. Machleidt, F. Sammarruca, and Y. Song, *Phys. Rev. C* **53**, R1483 (1995)
- [2] R. B. Wiringa, V. G. J. Stoks, and R. Schiavilla, *Phys. Rev. C* **51**, 38 (1995)
- [3] V. G. J. Stoks, R. A. M. Klomp, C. P. F. Terheggen, and J. J. de Swart, *Phys. Rev. C* **49**, 2950 (1994)
- [4] R. Machleidt, *Adv. Nucl. Phys.* **19**, 189 (1989)
- [5] R. Reid, *Ann. Phys. (N.Y.)* **50**, 411 (1968)
- [6] H. Müther, A. Polls, and W.H. Dickhoff, *Phys. Rev. C* **51**, 3040 (1995)
- [7] H. Müther, G. Knehr, and A. Polls, *Phys. Rev. C* **52**, 2955 (1995)
- [8] K.I. Blomqvist *et al.*, *Phys. Lett. B* **344**, 85 (1995)
- [9] K. Amir-Azimi-Nili, J.M. Udias, H. Müther, L.D. Skouras, and A. Polls, *Nucl. Phys. A* **625**, 633 (1997)
- [10] B.D. Serot and J.D. Walecka, *Adv. Nucl. Phys.* **16**, 1 (1986)
- [11] R. Brockmann and R. Machleidt, *Phys. Rev. C* **42**, 1965 (1990)
- [12] R. Fritz and H. Müther, *Phys. Rev. C* **49**, 633 (1994)
- [13] J.J. Kelly, *Adv. Nucl. Phys.* **23**, 75 (1996)

- [14] S. Ulrych and H. Müther, *Nucl. Phys. A* **641**, 499 (1998)
- [15] Contributions to this workshop by Elvira Maya de Guerra and Jose M. Udias
- [16] Contribution to this workshop by William Bertozzi
- [17] D. Knödler and H. Müther, preprint nucl-th/9812047
- [18] M. Vanderhaeghen, L. Machenil, J. Ryckebusch, and M. Waroquier, *Nucl. Phys. A* **580**, 551 (1994)
- [19] D. Knödler, H. Müther, and P. Czerski, work in progress
- [20] H. Kümmel, K. H. Lührmann, and J. G. Zabolitzky, *Phys. Rep.* **36**, 1 (1978)
- [21] R. F. Bishop, in *Microscopic Quantum Many-Body Theories and Their Applications*, eds. J. Navarro and A. Polls (Springer 1998)
- [22] J. G. Zabolitzky, *Nucl. Phys. A* **228**, 272 (1974)
- [23] C. Giusti, H. Müther, F. D. Pacati, and M. Stauf, preprint nucl-th/9903065
- [24] R. B. Wiringa, R. A. Smith, and T. L. Ainsworth, *Phys. Rev. C* **29**, 1207 (1984)
- [25] C. Giusti and F. D. Pacati, *Nucl. Phys. A* **571**, 694 (1994)
- [26] C. Giusti and F. D. Pacati, *Nucl. Phys. A* **641**, 297 (1998)
- [27] G. Rosner, *Proceedings of the 10th Mini-Conference on Studies of Few-Body Systems with High Duty-Factor Electron Beams*, NIKHEF, Amsterdam 1999, in press
- [28] J. R. M. Annand, P. Bartsch, D. Baumann, J. Becker, R. Böhm, D. Branford, S. Derber, M. Ding, I. Ewald, K. Föhl, J. Friedrich, J. M. Friedrich, P. Grabmayr (spokesperson), T. Hehl, D. G. Ireland, P. Jennewein, M. Kahrau, D. Knödler, K. W. Krygier, A. Liesenfeld, I. J. D. MacGregor, H. Merkel, K. Merle, P. Merle, U. Müller, H. Müther, A. Natter, R. Neuhausen, Th. Pospischil, G. Rosner (spokesperson), H. Schmieden, A. Wagner, G. J. Wagner, Th. Walcher, M. Weis, S. Wolf, MAMI proposal Nr: A1/5-98.
- [29] C. Giusti, F. D. Pacati, K. Allaart, W. J. W. Geurts, W. H. Dickhoff, and H. Müther, *Phys. Rev. C* **57**, 1691 (1998)
- [30] Contribution to this workshop by Carlotta Giusti

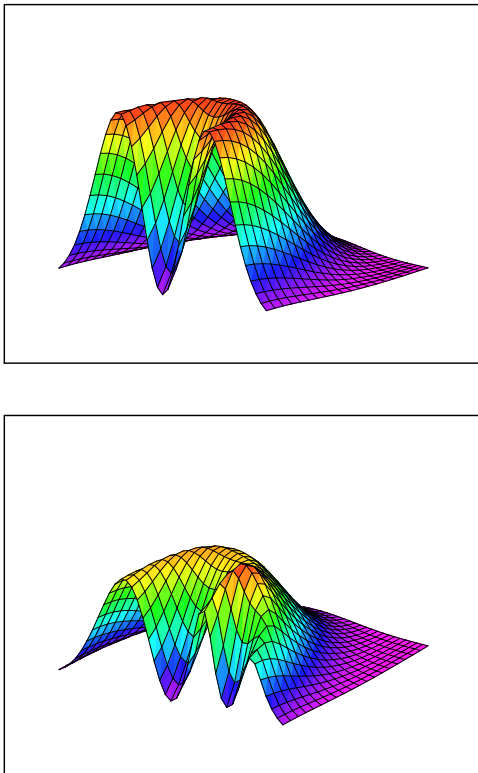


Figure 7: Two-body density according to (7) for a fixed vector \vec{r}_1 as a function of \vec{r}_2 . The upper part displays the result without correlations ($\hat{S}_2 = 0$), while correlations are included in the lower part of the figure. Further description in the text

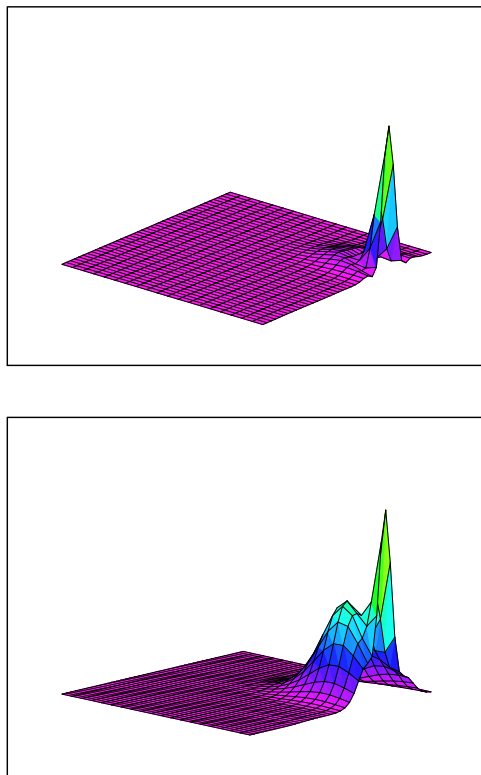


Figure 8: Correlation density according to (7) with ψ_2 replaced by \hat{S}_2 for a fixed vector \vec{r}_1 as a function of \vec{r}_2 . The upper part displays the result for a $J = 0, T = 1$ pair (pp) while the lower part refers to the removal of a $J = 1, T = 0$ (pn) pair.

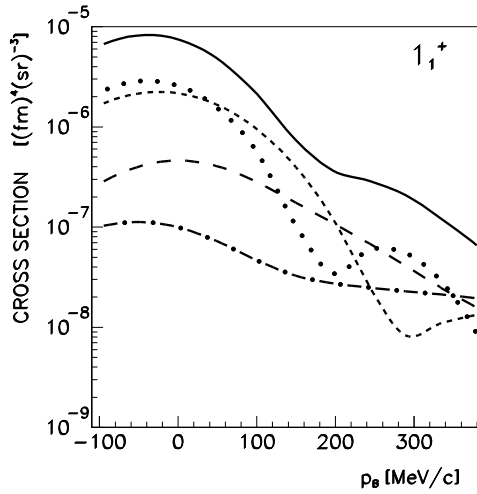


Figure 9: The differential cross section of the $^{16}\text{O}(\text{e},\text{e}'\text{pn})$ reaction as a function of the recoil momentum p_B for the transition to the 1_1^+ ground state of ^{14}N ($E_{2m} = 22.96$ MeV), in the super-parallel kinematics with $E_0 = 855$ MeV, and $\omega = 215$ MeV $q = 316$ MeV/c. The recoil-momentum distribution is obtained changing the kinetic energies of the outgoing nucleons. Separate contributions of the one-body, seagull, pion-in-flight and Δ -current are shown by the dotted, short-dashed, dot-dashed and long-dashed lines, respectively. Positive (negative) values of p_B refer to situations where p_B is parallel (antiparallel) to q .

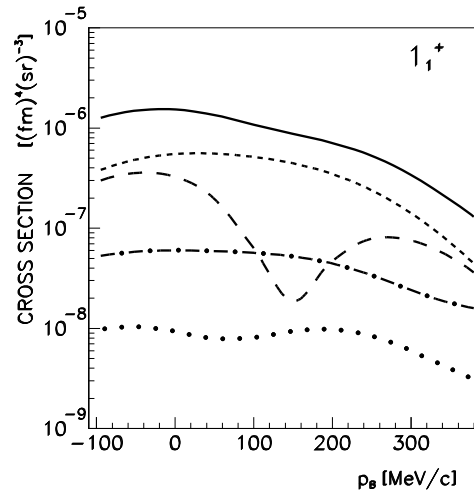


Figure 10: The same as Fig. 9 but with a simpler approach for the two-nucleon overlap.

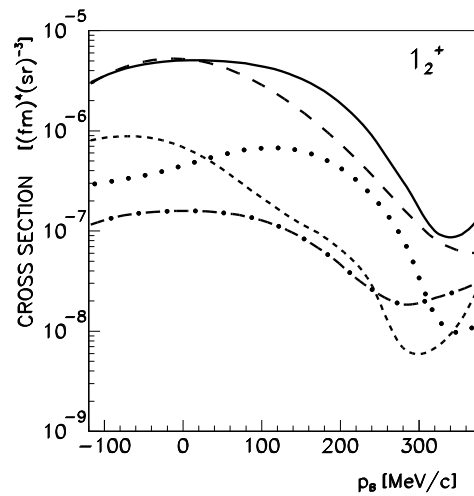


Figure 11: The same as Fig. 9 for the transition to the 1_2^+ state of ^{14}N ($E_{2\text{m}} = 26.91$ MeV).